Fermilab FERMILAB-Conf-02/299-E December 2002

Thermo-Mechanical Characterization of Insulated and Epoxy-Impregnated Nb_3Sn Composites

Linda Imbasciati, Giovanni Volpini, Giorgio Ambrosio, Deepak R. Chichili, Danilo Pedrini, Valentina Previtali, Lucio Rossi, Alexander V. Zlobin.

***Abstract*—Nb_3Sn is, at present, the best superconductor for high field accelerator magnets. Several models using Nb_3Sn are under development in many laboratories. Knowledge of the thermo-mechanical properties of the impregnated coils is of crucial importance for the design of these magnets. In fact, the performance of epoxy-impregnated coils is sensitive to the thermal conductivity value, especially in case of heating caused by hysteretic losses, which are usually relevant in Nb_3Sn magnets, and in the case of continuous heat deposition, such as in magnets near the interaction region of a collider. Thermal contraction measurements are necessary to estimate the stresses during the magnet thermal cycle. Different insulation materials have been studied at Fermilab utilizing various design approaches and fabrication methods. Thermal conductivity and thermal contraction measurements, at cryogenic temperatures, have been performed respectively at INFN-LASA and Fermilab. The results are reported and discussed in this paper.**

***Index Terms*—Nb_3Sn, superconducting coils, thermal conductivity measurement, thermal contraction measurements.**

I. Introduction

MANY high field accelerator magnets under development all over the world use Nb_3Sn superconductor and epoxy-impregnated coils. Fermilab is involved in the development of a cosine-theta dipole [1], of a single-layer common coil [2], and in the design of a low-beta quadrupole [3], using epoxy-impregnated Nb_3Sn coils. Also a common coil dipole model under development at LBNL [4], a block type dipole model at Texas A&M University [5], a large aperture dipole model at Twente University [6], and a LHC arc quadrupole-type model at CEA/Saclay [7] have this kind of coils. The knowledge of the thermo-mechanical properties of the impregnated coils is of crucial importance for the design of these and similar magnets. In fact, the performance of epoxy-impregnated coils is sensitive to the value of the thermal conductivity. This is particularly true in the case of heating caused by hysteretic losses, which are usually relevant in Nb_3Sn magnets because of their large effective filament diameter, and in the case of continuous heat deposition, such as in magnets near the interaction regions of a collider. Although the thermal properties of the individual materials forming the coils are well known, the resulting overall properties cannot be predicted with good accuracy.

Knowledge of the thermal contraction coefficients is necessary to estimate the stress redistributions occurring during magnet cool down and other thermal excursions.

Different insulations are under study at Fermilab for Nb_3Sn coils. A ceramic-fiber tape with ceramic binder insulation [8] is a key element of the FNAL cos-theta dipole. E-glass, Kapton® and pre-impregnated fiberglass tapes [9] have been studied during the R&D for FNAL single-layer common coil. The thermal expansion coefficient of ten-stack samples, with these insulations, was measured at Fermilab, and the thermal conductivity at cryogenic temperature of similar samples was measured at the INFN Laboratory for Applied Superconductivity and Accelerator (LASA) in Milan (Italy).

II. Description Of The Samples

The samples are stacks of reacted Rutherford cables, insulated, and vacuum impregnated with epoxy resin (CTD-101K) under a pressure of 15 MPa. The sample characteristics are listed in Table I.

TABLE I
SAMPLES PARAMETERS

Sample #	1	2	3	4 & 5
Insulation material	Fiberglass (E-glass) tape	Kapton+ pre-preg	Only epoxy	Ceramic fiber-tape
Ins. thickness, mm	0.2	0.23	-	0.35
Strand diameter, mm	0.7	0.7	0.7	1
Cu/non-Cu	1.4	0.87	0.87	0.92
Packing factor	0.87	0.87	0.87	0.9
Cable thickness, mm	1.2	1.2	1.2	1.8
Cable width, mm	14.5	14.5	14.5	14

Manuscript received August 6, 2002. This work was supported in part by the U.S. DOE under contract No. DE-AC02-76CH03000.

L. Imbasciati, G. Ambrosio, D. R. Chichili, and A. V. Zlobin are with Fermilab, Batavia, IL, 60510 USA (corresponding author phone: 630-840-6651; fax: 630-840-2383; e-mail: ilinda@fnal.gov).

D. Pedrini, V. Previtali, and G. Volpini are with University of Milan and with LASA/INFN-MI in Milan, ITA.

L. Rossi was with the University of Milan and LASA, and he is now with CERN.

The first sample is a 13 cables-stack, 86 mm long. All the other samples are ten-stacks, 25.4 mm long. The first three samples are stacks of cables with the same design (41 strands of 0.7 mm diameter). Similar cables were used for the construction of two racetrack magnets at Fermilab [10]. In the first sample, a fiberglass tape is wrapped around each cable with 30 % overlap. In the second sample, the turn-to-turn insulation consists of a layer of Kapton® tape (76 μm-thick), and a layer of pre-impregnated fiberglass tape (pre-preg). The final average thickness of the insulating layer, after impregnation, is 0.23 mm. The third sample is a stack of the same cable as in sample # 2, but it is epoxy-impregnated without any insulating material. The measure of its thermal conductivity, therefore, allows one to determine the contribution to the overall coil thermal conductivity of the insulating layer, and of the impregnated cable. The last two samples in Table I are ten-stacks of a cable with 28 strands, 1 mm in diameter, as the cable used in the Fermilab cos-theta dipole magnets. This cable has a higher compaction and higher copper content than the cable of samples # 2 and # 3. Samples # 4 and # 5, are prepared following the same procedure used for the production of the coils of the cos-theta dipole models. Each cable is wrapped with ceramic fibers tape, with 40 % overlap, then is wetted with a ceramic binder (CTD-1002x), and cured at 80 °C for 20 minutes. The samples are then heat treated to form the Nb_3Sn composite. Analysis at the SEM show that, after the heat treatment, the cable strands are coated with a thin layer of a material with a high content of oxygen and silica [11]. The effect of this coating on the contact resistance between the strands is under investigation at Fermilab.

III. Conductivity Measurements

A. Measurement Set-Up

The experimental setup, described in detail in [12] is briefly presented here. The basic method of the measurement is a steady-state method: the sample is placed between two heat sinks, providing a constant heat flux, in one (axial) dimension, when thermal equilibrium is reached. The cold sink is in direct contact with the cryogen, and the warm sink is heated with an electrical heater. The measures of the current and of the voltage across the resistor provide a precise value of the input power. The heat flux is then given by the power divided by the area of the cross section of the sample.

The temperature is measured at several points along the sample and on the two sinks, through Au-Fe (0.07 % at w.) - Chromel P thermo-couples. The system is enclosed in a vacuum chamber in which the pressure is maintained at about 10^{-6} mbar, to avoid convective losses. The vacuum chamber is made of stainless steel, and is gold plated to reduce radiative losses. The main parts of the apparatus are shown in Fig. 1.

B. Measurement Analysis

The Fourier-Biot law determines the thermal conductivity:

$$\dot{Q} = -k(T) \cdot S \cdot dT/dl \ , \tag{1}$$

where $\dot{Q} = -P$ is the heat flowing in the sample (equal to the input power P, but in opposite direction with respect to the temperature differential dT/dl); k is the thermal conductivity (which is temperature dependent); and S is the cross-sectional area of the sample. Considering S a constant, and approximating k to a linear function of temperature, we calculate the thermal conductivity at an average temperature $T_{AVE} = (T_2 + T_1) / 2$, with $\Delta T = T_2 - T_1$, through the equation:

$$k(T_{AVE}) = P \cdot l / (S \cdot \Delta T). \tag{2}$$

The approximation of $k(T)$ as a linear function is a good approximation for metals at low temperature, or if the conductivity dependence from temperature is a slowly varying function. The conductivity of the insulating materials instead, has typically a steep increase at low temperature. In the case of our composite samples, at temperature close to liquid Helium temperature, the error due to this approximation, when the considered temperature differences are of few Kelvin, can induce an overestimation less than a few percent.

Another source of error is the power loss, due to heat dissipated by convection through the supporting system, convective losses through residual gas, and radiation from the warm sample and from the heater to the vacuum vessel at bath temperature. The setup is designed and tested to have very low power losses, estimated to be about 3 % of the input power, in most of the temperature range of operation with liquid Helium. A maximum dissipation of 10 % is possible using liquid nitrogen, due to larger temperature differences.

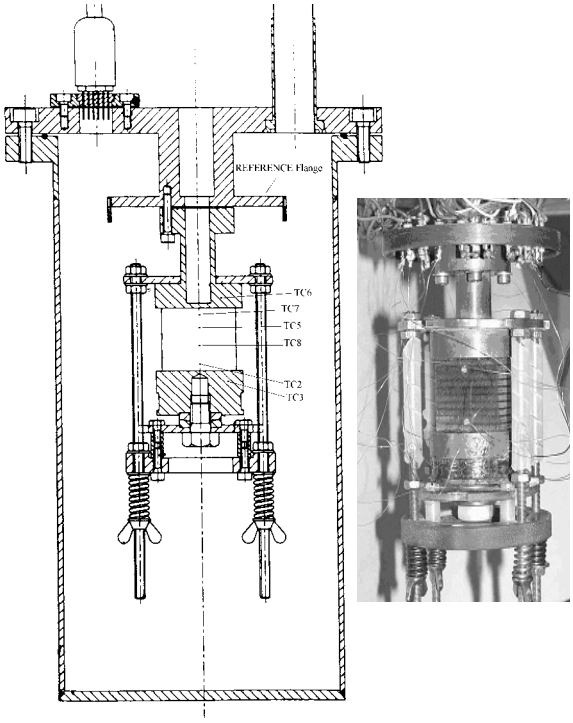

Fig. 1. Schematic drawing and picture of the conductivity measurement sample holder inside the vacuum chamber. TC2, … TC8 indicate the thermocouple positions.

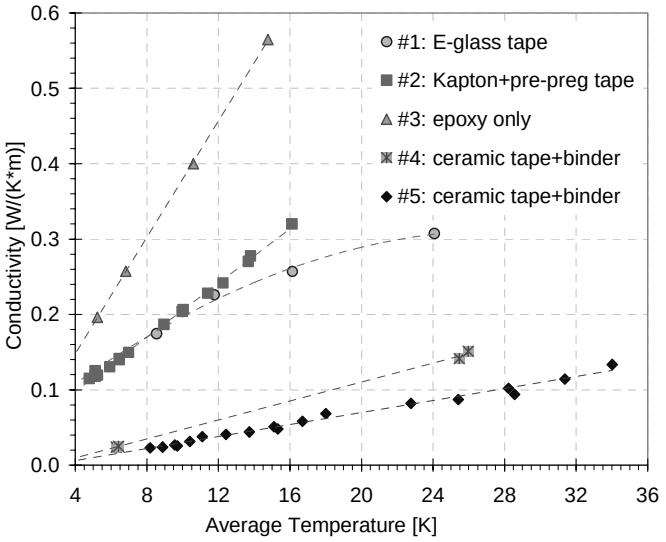

Fig. 2. Results of the conductivity measurements with liquid Helium: experimental data (points) and interpolating functions (dashed lines).

C. Conductivity Measurements Results

Fig. 2 and 3 show the results of the conductivity measurements performed using liquid Helium and liquid Nitrogen as cryogens, respectively. The measured data from sample #1 (E-glass insulation) can be interpolated using a quadratic function, while all the other data of Fig. 2 can be interpolated using linear functions. The conductivity values of sample #1 and #2 are close, at temperatures below 12 K. The extrapolated value at 4.2 K is 0.1 W/(K·m). Sample #3 (epoxy impregnated without insulation) has a higher thermal conductivity, than the insulated samples, with an extrapolated value at 4.2 K of 0.16 W/(K·m). Samples #4 and #5 (ceramic insulation) have a very low thermal conductivity of 0.03 W/(K·m), at 6 and 8 K respectively. Extrapolation to lower temperatures might result in an underestimation of the real conductivity, since the linear interpolating functions have a small, but negative value at zero Kelvin.

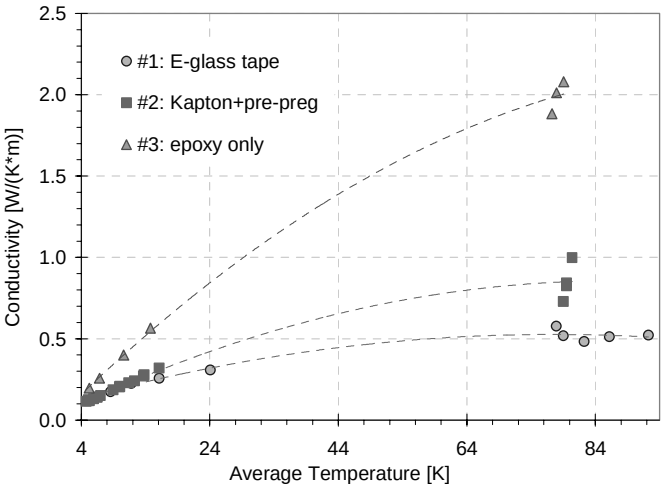

Fig. 3. Results of the conductivity measurements with liquid Nitrogen: experimental data (points) and a quadratic interpolation of the experimental data (dashed lines).

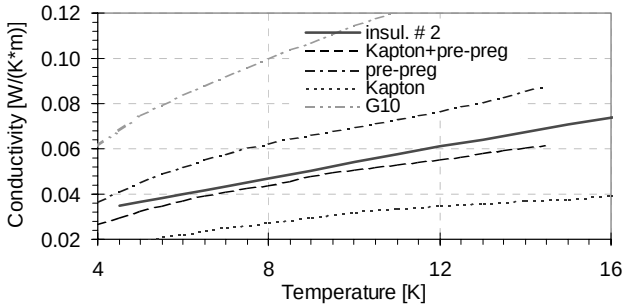

Fig. 4. Thermal conductivity of sample # 2 insulation, consisting of Kapton and pre-preg tape, compared with other insulating materials.

The thermal conductivity of the Kapton plus pre-preg insulation was calculated subtracting the contribution of the impregnated cable (sample #3), from the thermal resistance of sample #2. In Fig. 4, the continuous line indicates the resulting thermal conductivity, compared with the thermal conductivity of other insulating materials: G10 [13], Kapton, and pre-preg [14], [15]. The thermal conductivity resulting from 76 μm Kapton plus 0.154 mm pre-preg agrees within 10 % with the conductivity of sample #2 insulation.

In a first approximation, the conductivity of the cable stacks can be calculated using a simple model, where the composite is approximated by a series of thermal resistances. The fractions of the components are weighted over the cable cross section. Fig. 5 shows the results of the calculations for sample #1, using pre-preg ([14], [15]) as turn-to-turn insulation. The two lines of Fig. 5 represent the calculated conductivity, including and not including the epoxy fraction (continuous and dashed lines respectively). A more detailed analysis should also consider the thermal contact resistance between the two layers of strands of the Rutherford cable, and the effect of the transposition pitch. The contact thermal resistance is very difficult to evaluate, since it depends on the contact surface area and on other insulating materials that can cover the strands, such as oxides and epoxy. In addition, samples #1-3 are fabricated following the procedure of the racetrack magnet, which includes synthetic oil, in order to prevent sintering of the two layers of strands during reaction. Sample #4 and 5 might have a ceramic coating. The difference in the conductivity between the samples can be explained by a difference in the thickness of the coating or in the pressure during preparation.

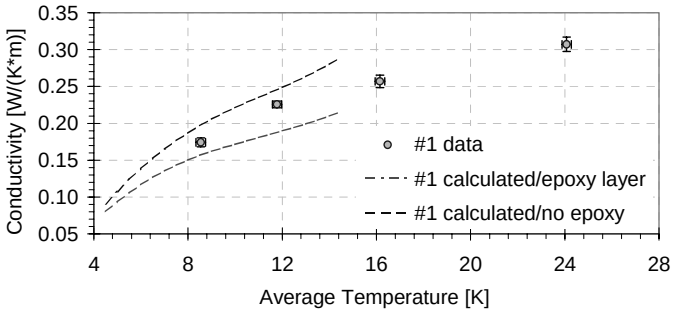

Fig. 5. Comparison of the measured thermal conductivity data with the thermal conductivity calculated from the material properties of the components, for sample #1 (E-glass insulation).

IV. Thermal Contraction Measurements

Measurements of the integrated thermal contraction from 293 K to 77 K were performed using calibrated strain gauges. The technique, described in details in [16], was used before at Fermilab for the measurements of samples # 4 and 5 [17].

A temperature change ΔT induce a resistance change ΔR, due to 1) a change in the resistivity of the grid material, that proportional to the thermal coefficient β_G; 2) a difference in the thermal contraction coefficients between the sample and the grid, α_S and α_G respectively. The relative resistance change of the gage on a sample is given by the sum of these two effects:

$$\Delta R_S / R = [\beta_G + (\alpha_S - \alpha_G) \cdot F_G] \cdot \Delta T = \varepsilon_S \cdot F_G, \quad (3)$$

where F_G is the gage factor, a proportionality factor between the apparent strain ε, and the relative resistance change. If the same type of gage is installed on a standard reference material with a known thermal coefficient α_R, then

$$\Delta R_R / R = [\beta_G + (\alpha_R - \alpha_G) \cdot F_G] \cdot \Delta T = \varepsilon_R \cdot F_G, \quad (4)$$

Subtracting the above two equations and rearranging, we get

$$(\alpha_s - \alpha_R) = (\varepsilon_s - \varepsilon_R) / \Delta T. \quad (5)$$

Knowing α_R, ε_S and ε_R for a particular change in temperature, we can compute α_S, the integrated thermal contraction coefficient of the sample.

The thermal contraction was measured in two directions: vertical direction, which corresponds to the azimuthal direction in a cos-theta dipole magnet, and the horizontal direction corresponding to the radial direction in the magnet. Two different types of gauges (Gauge - 1 and Gauge - 2 in Table II) of the WK Series from Micro Measurements Group were installed in each direction, to check for repeatability and for gauge-type errors. Measurement results are reported in Table II. The first sample of the Table II is sample #2 of Table I. Two other ten-stacks were made using the same cable, but with different insulation. Data of samples #4 and 5, reported in [17], are listed here for comparison.

TABLE II
Integrated Thermal Contraction Data From 293 K To 77 K

Vertical (Azimuthal) Thermal Contraction			
Insulation Pattern	Gauge - 1	Gauge - 2	Average
Kapton + E-glass	4.262	4.045	4.154
Kapton (0.2 mm)	4.419	4.606	4.513
E-glass (0.18 mm)	3.646	3.77	3.708
Ceramic-fibers			3.22
Horizontal (Radial) Thermal Contraction			
Insulation Pattern	Gauge - 1	Gauge - 2	Average
Kapton (0.2 mm)	2.808	2.904	2.856
Kapton + E-glass	3.000	2.966	2.983
E-glass (0.18 mm)	2.970	2.996	2.983
Ceramic-fibers			2.29

Data in mm/m.

The readings of the two gauges are consistent. To confirm the technique adopted, one of the types of gauges used on the ten-stacks was used on a copper and a stainless steel sample, and the measured data were compared with published values. The measured integrated thermal coefficient (from 293 K to 77 K) of 304 SS and copper samples, are 2.85 and 3.07 mm/m respectively, very close to the published values of 2.81 and 3.07 mm/m.

In the radial direction, as expected, the integrated thermal contraction coefficient does not depend on the insulation pattern. However, this value is higher than the previously measured value for the 28 strands, 1.0 mm diameter cos-theta cable (α_S = 2.29 mm/m). In azimuthal direction, the integrated thermal contraction coefficient depends on the insulation pattern, varying from 3.2 to 4.5 mm/m. Measurements performed on similar cable stacks, insulated with quartz fibers, are within this range (α = 3.9 mm/m) [18].

References

[1] N. Andreev et al., "Development and Test of a Single-bore cosθ Nb_3Sn Dipole Models with Cold Iron Yoke," *IEEE Trans. Applied Superconductivity*, Vol. 12, no. 1, pp 332-336.

[2] G. Ambrosio et al., "R&D for a Single-Layer Nb_3Sn Common Coil Dipole Using the React-and-Wind Fabrication Technique," *IEEE Trans. Applied Superconductivity* Vol. 12, no. 1, pp 39-42.

[3] A.V. Zlobin et al. "Conceptual Design Study of Nb_3Sn Low-Beta Quadrupoles for 2nd Generation LHC IRS," presented at this conference, 2LC-04.

[4] A.F. Lietzke et al., "Test Results for RD3c, a Nb_3Sn Racetrack Dipole Magnet", presented at this conference, 3LA-05.

[5] P.M. McIntyre et al., "Construction and Testing of Block-coil High-field Dipoles for Future Hadron Colliders," presented at this conference, 4LC-04.

[6] A. den Ouden et al., "Component Properties of the 1 Meter 10 T Nb_3Sn Dipole Magnet," presented at this conference, 3LA-04.

[7] A. Devred, et al., "Development of a Nb_3Ssn Quadrupole Magnet Model," presented at ASC 2000, Virgina Beach, USA, 09-2000.

[8] D. R. Chichili et al., "Fabrication and testing of High Field Dipole Mechanical Model," MT-16, Tallahassee, FL, 1999.

[9] G. Ambrosio et al., "Study of insulating materials for HFDB-02 Racetrack Magnet using Nb_3Sn and the react-and-wind technology," Fermilab TD note, TD-02-008, March 2002.

[10] G. Ambrosio et al., "Fabrication and Test of a Racetrack Magnet Using Pre-Reacted Nb_3Sn Cable," presented at this conference, 3LA-03.

[11] M. Barzi et al., "Development and study of Rutherford-type Cables for Accelerators Magnets at Fermilab," presented at this conference.

[12] F. Broggi, S. Piuri, L. Rossi, "An apparatus for thermal conductivity measurements at cryogenic temperature on coil blocks," INFN/TC-93/01, 1993.

[13] Cryocomp v 2.0, Eckels Engineering and Cryodata Inc., normal to cloth G10 properties.

[14] F. Rondeaux, Ph. Bredy, J.M. Rey, CEA Saclay, "Thermal Conductivity Measurements of Epoxy Systems at Low Temperature," Advances in Cryogenic Engineering Materials, Vol. 48A, pg 197.

[15] M. Damasceni, L. Rossi, S. Visona, "Measurements at cryogenic Temperature of the Thermal Conductivity of the ground Insulation of a Model of the ATLAS BT coils," tech. Rep. LASA/ATLAS/510 (1998)

[16] MICRO MEASUREMENTS GROUP, Strain Gage Technology: Thermal Expansion Measurement, Tech. Rep. TN-513.

[17] D. R. Chichili et al., "Investigation of cable insulation and thermo-mechanical properties of Nb3Sn composite," *IEEE Trans. Appl. Supercond.*, Vol. 10 N. 1, pp 1317-1320, 2000.

[18] M. Reytier et al., "Characterization of the Thermo-Mechanical Behavior of Insulated Cable Stacks Representative of Accelerator Magnet Coils", *IEEE Trans. Appl. Supercond.*, Vol. 11 N. 1, 2001.